Crystal Structures and Luminescence Properties of $[Ln(NTA)_2 \cdot H_2O]^{3-}$ Complexes (Ln = Sm^{3+}, Eu^{3+}, Gd^{3+}, Tb^{3+}, Ho^{3+}, and NTA = Nitrilotriacetate)

Jun-Gill Kang,* Hee-Jung Kang, Jae-Sun Jung, Sock Sung Yun, and Chong-Hyeak Kim†

Department of Chemistry, Chungnam National University, Daejeon 305-764, Korea
†Korea Research Institute of Chemical Technology, P.O. Box 107, Daejeon 305-600, Korea
Received March 16, 2004

Crystal structures of lanthanide complexes with NTA (NTA = nitrilotriacetate) are reported. The complexes of $[Ln(NTA)_2 \cdot H_2O]^{3-}$ (Ln = Sm, Eu, Gd, Tb and Ho) crystallize in the orthorhombic space group *Pccn*. In the structures, the trivalent lanthanide ions are completely encapsulated via coordination to the two nitrogen atoms and the six carboxylate oxygen atoms of the two NTA ligands, and one water oxygen atoms. The complexes form a slightly distorted capped-square-antiprism polyhedron. Of the complexes, $[Eu(NTA)_2 \cdot H_2O]^{3-}$, $[Tb(NTA)_2 \cdot H_2O]^{3-}$ and $[Dy(NTA)_2 \cdot H_2O]^{3-}$ excited at the 325 He-Cd line produce very characteristic luminescence features, arising mostly from the f $\rightarrow$ f transitions. The absolute quantum yields of these complexes are determined at room temperature. Surprisingly, the $[Dy(NTA)_2 \cdot H_2O]^{3-}$ complex is more luminescent than the $[Eu(NTA)_2 \cdot H_2O]^{3-}$ and $[Tb(NTA)_2 \cdot H_2O]^{3-}$ complexes.

Key Words : Rare earth complexes, Crystal structure and symmetry, Luminescence, Quantum yield

Introduction

Recently, the coordination chemistry of NTA with lanthanide ions has drawn much attention, since lanthanide complexes with NTA exhibit unprecedently high acceleration factors in the hydrolysis of phosphate ester[1] and a high selectivity for the separation of rare-earth elements.[2,3] However, to our knowledge, the molecular structures of only three lanthanide-NTA complexes have been reported: $[Pr \cdot NTA] \cdot 3H_2O$,[4] $[Dy \cdot NTA] \cdot 4H_2O$[5] and $[Tm \cdot NTA \cdot (H_2O)_2]$[6]. Generally, It has been found that lanthanide ions form 1 : 1 complexes with NTA, although their coordination numbers range from 6 to 12 in various complexes. The uncertainty about the Ln(III) metal-binding capability of NTA and the molecular geometry of the lanthanide complex prompted us to undertake this study. Its aim is to characterize the molecular structure of Ln(III)/NTA (Ln = Sm, Eu, Gd, Tb and Ho) in detail. In addition, we have reported the luminescence properties of these complexes as well as Dy/NTA and compared their quantum yields.

Experimental Section

Crystal growth and composition analysis. Synthesis of $[Ln(NTA)_2 \cdot H_2O]^{3-}$ (Ln = Sm, Eu, Gd, Tb, Ho). $LnCl_3 \cdot 6H_2O$ (Aldrich) and disodium nitriloacetate (Na_2NTAH, Aldrich) were of analytical grade and used without further purification. The mother solution was prepared by mixing 0.50 M Ln(III) and 0.50 M Na_2NTAH solutions in a 1 : 2 molar ratio of Ln(III) to NTA. The pH of the solution was adjusted to between 5 and 6 with dilute KOH. Colorless microcrystals of Ln(III) complex with NTA were obtained by the slow evaporation method. The cations were analyzed quantitatively with an ICP spectrophotometry (Jovin Yvon JY-50P), and the total organic carbon (TOC) was determined on an Astro-2001 Analyzer. A potentiometric analysis also showed that there were no chloride ions in the crystals. Anal. Found: K 16.7; Sm 20.4; C 19.9; H 3.5; N 4.0, Cal. for $K_3[Sm(NTA)_2(H_2O)] \cdot 5.5H_2O$: K 15.4; Sm 19.8; C 18.9; H 3.3; N 3.7%. Anal. Found: K 15.5; Eu 20.1; C 19.3; H 3.3; N 3.9, Cal. For $K_3[Eu(NTA)_2(H_2O)] \cdot 5.5H_2O$: K 15.4; Eu 19.9; C 18.9; H 3.3; N 3.7 %. Anal. Found: K 15.0; Gd 21.0; C 19.6; H 3.4; N 3.9, Cal. for $K_3[Gd(NTA)_2(H_2O)] \cdot 5.5H_2O$: K 15.3; Gd 20.5; C 18.8; H 5.2; N 3.6 %. Anal. Found: K 4.89; Na 7.03; Tb 22.4; C 19.05; H 3.31; N 3.81; O 39.51%. Cal. for $KNa_2[Tb(NTA)_2(H_2O)] \cdot 5.5H_2O$: K 5.30; Na 6.24; Tb 21.55; C 19.55; H 3.42; N 3.80; O 40.14%. Anal. Found: K 16.0; Ho 22.8; C 19.5; H 3.3; N 3.9; O 28.1. Cal. for $K_3[Ho(NTA)_2(H_2O)] \cdot 5.5H_2O$: K 15.1; Ho 21.3; C 18.6; H 3.3; N 3.6%.

Determination and refinement of the X-ray structure. Intensity data were collected at room temperature on a Bruker P4 diffractometer using graphite monochromated Mo Kα radiation. The intensities were corrected for Lorentz-polarization effects, and empirical absorption correction (Ψ scan) was also applied. The structures of the titled compounds were solved by applying the direct method using a Bruker SHELXTL[7] and refined by a full-matrix least-squares refinement on F using SHELEX97.[8] The non-H atoms were refined with anisotropic displacement parameters. Weights were assigned as $w = 1/[\sigma^2(F_0^2) + (aP)^2 + bP]$ where $P = (F_0^2 + 2F_c^2)/3$. The values of *a* and *b* are 0.0905 and 31.4488 for Sm/NTA, 0.0792 and 35.2951 for Eu/NTA, 0.0752 and 43.2933 for Gd/NTA, 0.0615 and 22.1217 for Tb/NTA, and 0.0771 and 47.2806 for Ho/NTA, respectively. The crystal data and refinement results are summarized in Table 1.

Optical measurements. For photoluminescence (PL) and

*To whom all correspondence should be addressed. e-mail: jgkang@cnu.ac.kr

Table 1. Crystallographic data and refinements for $[Ln(NTA)_2 \cdot H_2O]^{3-}$ complexes

	1	**2**
chemical formula	$C_{12}SmH_{25}K_3N_2O_{18.5}$	$C_{12}EuH_{25}K_3N_2O_{18.5}$
formula weight	760.99	762.60
T(K)	288(2)	288(2)
crystal system	orthorhombic	orthorhombic
space group	*Pccn*	*Pccn*
a(Å)	16.275(90)	16.273(90)
b(Å)	19.749(90)	19.744(90)
c(Å)	14.8973(90)	14.863(90)
V(Å^3)	4788.2(13)	4775.3(11)
Z	8	8
ρ_{cal}(mg/m^3)	2.111	2.121
μ (mm^{-1})	3.065	3.241
F(000)	3024	3032
theta range (^{o})	2.06 - 26.50	2.06 - 26.50
limiting index	$-1 \le h \le 20$, $-1 \le k \le 24$, $-1 \le l \le 18$	$-1 \le h \le 20$, $-1 \le k \le 24$, $-1 \le l \le 18$
reflections collected/unique	6063/4969[R(int) = 0.0352]	6032 / 4945 [R(int) = 0.0224]
max. and min. transmission	0.3101 and 0.2252	0.2726 and 0.2325
data/restraints/parameters	4969/0/330	4945 /0/ 330
goodness-of-fit on F^2	1.065	1.078
final *R* indices [I>2σ(I)]	R_1 = 0.0516, wR_2 = 0.1508	R_1 = 0.0462, wR_2 = 0.1439
R indices (all data)	R_1 = 0.0637, wR_2 = 0.1613	R_1 = 0.0500, wR_2 = 0.1473

3	**4**	**5**
$C_{12}GdH_{25}K_3N_2O_{18.5}$	$C_{12}TbH_{25}KNa_2N_2O_{18.5}$	$C_{12}HoH_{25}K_3N_2O_{18.5}$
767.89	737.34	775.57
293(2)	295(2)	290(2)
orthorhombic	orthorhombic	orthorhombic
Pccn	*Pccn*	*Pccn*
16.282(90)	16.251(90)	16.261(90)
19.777(90)	19.727(90)	19.754(90)
14.870(90)	14.784(90)	14.7566(90)
4788(3)	4739.4(17)	4740.1(11)
8	8	8
2.130	2.067	2.147
3.382	3.288	3.957
3040	2920	3064
2.06-26.49	2.06-27.51	2.06-26.49
$-1 \le h \le 20$, $-24 \le k \le 1$, $-1 \le l \le 18$	$-21 \le h \le 1$, $-1 \le k \le 25$, $-1 \le l \le 19$	$-1 \le h \le 20$, $-1 \le k \le 24$, $-18 \le l \le 1$
5364/4361 [R(int) = 0.0237]	6604/5441 [R(int) = 0.0297]	4541/3664 [R(int) = 0.0295]
0.3136 and 0.2346	0.3006 and 0.2628	0.3341 and 0.2189
4361 /0/ 330	5441 /0/ 330	3664 /0/ 330
1.102	1.123	1.119
R_1 = 0.0475, wR_2 = 0.1426	R_1 = 0.0450, wR_2 = 0.1236	R_1 = 0.0469, wR_2 = 0.1431
R_1 = 0.0550, wR_2 = 0.1497	R_1 = 0.0488, wR_2 = 0.1266	R_1 = 0.0556, wR_2 = 0.1505

$R = \Sigma \, | \, |F_0| - |F_c| \, | \, / \, \Sigma \, |F_0|$

excitation spectra measurements single crystals were placed on the cold finger of a CTI-cryogenics using silicon grease. The spectra were measured at a 90^o angle with an ARC 0.5 m Czerny-Turner monochromator equipped with a cooled Hamamatsu R-933-14 PM tube. The sample was irradiated with a He-Cd 325-nm laser line or the light from an Oriel 1000 W Xe lamp (working power, 400 W) passing through an Oriel MS257 monochromator.

The absolute quantum yield, *Q*, defined by

$$Q = \frac{\text{number of photons emitted}}{\text{number of photons absorbed}},$$

was measured with a custom-built integrating sphere (Lapshere). The sphere 10 cm in diameter is a hollow sphere,

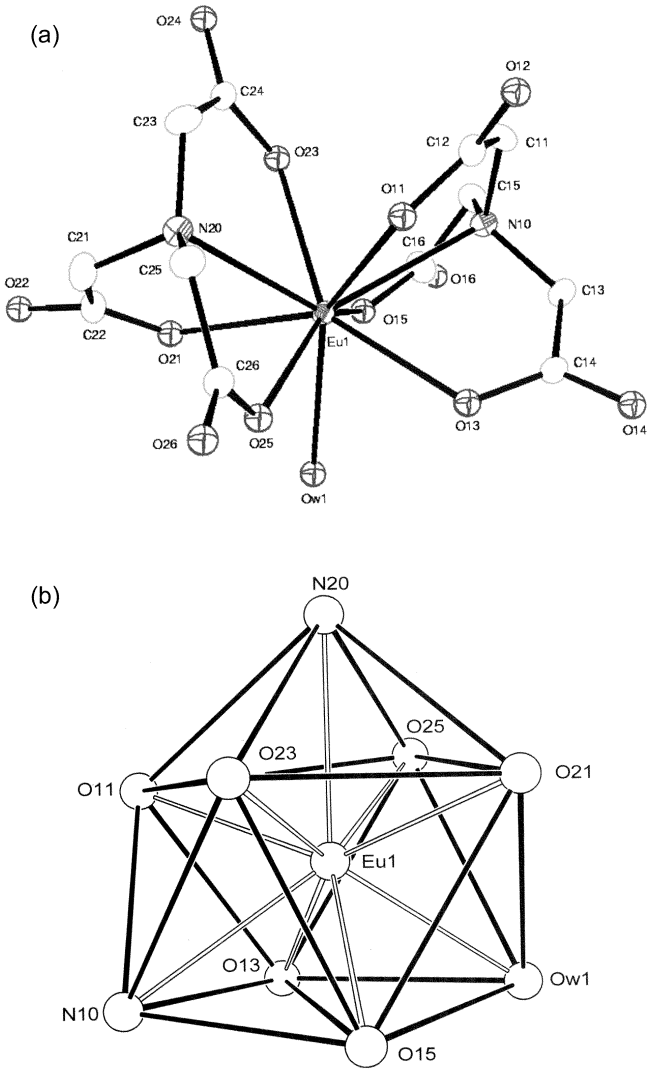

Figure 1. (a) ORTEP drawing and the atom-labeling schemes and (b) ORTEP view of coordination sites of $[Eu(NTA)_2 \cdot H_2O]^{3-}$. The displacement ellipsoids are drawn at the 40% probability level and the hydrogen atoms are omitted in ORTEP drawing for clarity.

coated on the inside with diffusely reflecting materials. The experimental details were described by Mello *et al.*.[9] The output of the sphere was directed into the monochromator and the recorded spectra were corrected for the spectral response of the system using an Oriel 45 W quartz tungsten halogen lamp standard. All measurements were repeated 3 times.

Results and Discussion

Coordination and polyhedron. The complexes crystallize as the orthorhombic space group *Pnaa* ($Z = 8$). The typical ORTEP view of the $[Ln(NTA)_2(H_2O)]^{3-}$ molecular unit is shown in Figure 1. Selected bond lengths and angles are given in Table 2. It has been argued that NTA forms 1 : 1 complexes with most of metal ions including trivalent lanthanide ions, as seen in $[Pr \cdot NTA] \cdot 3H_2O$[4], $[Dy \cdot NTA] \cdot 4H_2O$[5] and $[Tm \cdot NTA \cdot (H_2O)_2]$[6]. For $[Pr \cdot NTA] \cdot 3H_2O$, NTA satisfies heptadentate form with six carboxylate oxygen atoms and one nitrogen atom. For $[Dy \cdot NTA] \cdot 4H_2O$ and $[Tm \cdot NTA \cdot (H_2O)_2]$, each NTA is hexadentate with five carboxylate oxygen atoms and one nitrogen atom as in the case of [PrNTA] complex, while one carboxylate oxygen atom is not coordinated to any metal atom. The molecular structures of the titled complexes are certainly different from those lanthanide complexes. Unexpectedly, the Ln(III) ions form complexes with a 1 : 2 ratio of metal to NTA, as shown in Figure 1. In the titled complexes, NTA acts as a tetradentate ligand. Each NTA forms three five-membered chelated rings through the nitrogen atom. The rare earth ions are completely encapsulated by six pendant arms and one water molecule. The comparative results listed in Table 3 for Ln-NTA systems exhibit some expected behavior across the lanthanide series. One can note that if Dy-NTA is excluded from consideration, then the average bond lengths decrease across the series. It can be rationalized in terms of the relative ionic radius of lanthanide ion, *i.e.*, as the ion radius of Ln(III) decreases, the bond lengths decrease across the series.

The idealized structures for the 9 coordinate complexes are the tricapped trigonal prism (TCTP) and the capped square antiprism (CSAP) polyhedra.[10] Nine-coordinated Ln(III) complexes most frequently form the TCTP polyhedron, while the CSAP polyhedron is very rare.[11] In Fig. 1(b), the TCTP geometry can be accessed by the three rectangular (O13-O15-O21-O25, O13-O15-O23-O11, O11-O23-O21-O25) and the two triangular (O13-O11-O25, O15-O23-O21) faces of the trigonal prism and the three atoms occupying the capping positions (N20, Ow1, N10). Alternatively, the CSAP geometry can be described by the two rectangular faces of the square antiprism (O11-O23-O21-O25, N10-O15-Ow1-O13) and the N20 atom occupying the capping position. The shape of the nine-coordinate polyhedron can be accessed by calculating the dihedral angles (δ) between pairs of adjacent triangular faces: Ow1(O13O15)-N10, N10(O11O23)N20 and N20(O21O25)Ow1. The respective determined angles for the titled complexes are ranged in 8.8-9.2°, 26.2-27.4° and 25.9-27.9°, respectively. The most significant difference in the dihedral angle between the TCTP and the CSAP geometries can be found in Ow1(O13O15)N10 with δ = 8.8-9.2°. In the case of the structures of ideal ML_9 monomers, this δ angle in the TCTP geometry is in the range of 25°-30°, while in the CSAP geometry, it is 0°.[10] This dihedral angle indicates that Ow1, O13, N10 and O15 may be almost planar. Accordingly, the geometries of the titled complexes are very close to the CSAP rather than the TCTP. In the CSAP, the two rectangular planes, (O11-O23-O21-O25) and (N10-O15-Ow1-O13), are slightly declined with a torsion angle of 3.34-4.40°. The O11 and O21 atoms are located 0.078-0.087 and 0.082-0.092 Å above their mean plane, respectively, while the O23 and O25 atoms are displaced in the opposite direction by 0.084-0.095 and 0.082-0.092 Å, respectively. The O15 and O13 atoms are located 0.088-0.092 and 0.077-

Table 2. Selected bond lengths (Å) and angles (°) for [Ln(NTA)$_2$·H$_2$O]$^{3-}$ complexes

	1	**2**	**3**	**4**	**5**
Ln-O23	2.407(5)	2.391(5)	2.386(5)	2.363(4)	2.356(6)
Ln-O13	2.401(5)	2.394(4)	2.386(5)	2.367(4)	2.348(6)
Ln-O25	2.426(5)	2.414(4)	2.404(5)	2.388(4)	2.377(6)
Ln-O15	2.433(5)	2.419(4)	2.413(5)	2.388(4)	2.373(7)
Ln-O11	2.443(5)	2.422(5)	2.408(6)	2.394(4)	2.371(6)
Ln-O21	2.439(5)	2.425(5)	2.418(5)	2.398(4)	2.370(6)
Ln-OW1	2.543(5)	2.531(5)	2.524(6)	2.516(4)	2.495(6)
Ln-N20	2.656(6)	2.648(5)	2.642(6)	2.633(4)	2.615(8)
Ln-N10	2.688(5)	2.683(5)	2.672(6)	2.665(4)	2.649(7)
O23-Ln-O13	140.46(18)	140.40(16)	140.17(19)	140.65(14)	140.5(2)
O23-Ln-O25	128.81(16)	129.19(15)	129.47(18)	129.47(12)	130.4(2)
O13-Ln-O25	77.51(17)	77.40(15)	77.38(18)	77.00(13)	76.7(2)
O23-Ln-O15	77.11(17)	77.16(15)	77.12(18)	77.56(13)	77.3(2)
O13-Ln-O15	95.42(18)	95.20(15)	95.01(19)	94.97(13)	94.9(2)
O25-Ln-O15	145.70(17)	145.34(15)	145.28(18)	144.77(13)	143.9(2)
O23-Ln-O11	82.08(19)	82.10(17)	82.2(2)	82.29(14)	82.4(2)
O13-Ln-O11	71.88(19)	72.16(17)	72.2(2)	72.51(14)	72.8(2)
O25-Ln-O11	82.74(18)	82.61(16)	82.42(19)	82.09(14)	82.3(2)
O15-Ln-O11	127.40(17)	127.81(15)	127.94(18)	128.71(13)	129.2(2)
O23-Ln-O21	75.2(2)	75.17(18)	75.2(2)	75.17(16)	75.4(2)
O13-Ln-O21	142.80(18)	142.74(17)	142.71(19)	142.23(14)	142.0(2)
O25-Ln-O21	84.79(19)	85.13(17)	85.6(2)	85.96(15)	86.1(2)
O15-Ln-O21	81.13(17)	80.80(16)	80.44(19)	79.84(14)	79.3(2)
O11-Ln-O21	138.14(18)	138.09(16)	138.4(2)	138.50(14)	138.6(2)
O23-Ln-OW1	133.65(19)	133.81(17)	133.9(2)	134.16(14)	134.2(2)
O13-Ln-OW1	73.89(17)	73.60(15)	73.44(18)	72.85(13)	72.8(2)
O25-Ln-OW1	78.21(17)	77.86(16)	77.90(19)	77.71(14)	76.7(2)
O15-Ln-OW1	67.64(17)	67.62(15)	67.51(19)	67.19(13)	67.3(2)
O11-Ln-OW1	143.62(18)	143.46(17)	143.3(2)	142.94(14)	142.9(2)
O21-Ln-OW1	70.58(17)	70.65(16)	70.65(19)	70.69(14)	70.3(2)
O23-Ln-N20	65.57(17)	65.87(16)	66.00(18)	66.03(13)	66.5(2)
O13-Ln-N20	128.63(18)	128.73(16)	129.13(19)	128.98(14)	129.0(2)
O25-Ln-N20	63.24(17)	63.32(15)	63.47(18)	63.45(13)	63.9(2)
O15-Ln-N20	135.62(17)	135.78(16)	135.61(18)	135.87(13)	135.9(2)
O11-Ln-N20	71.51(19)	71.34(17)	71.7(2)	71.34(14)	71.0(2)
O21-Ln-N20	67.18(18)	67.34(16)	67.31(19)	67.75(14)	68.1(2)
OW1-Ln-N20	124.06(16)	123.90(15)	123.77(18)	123.82(13)	123.4(2)
O23-Ln-N10	74.98(17)	74.80(16)	74.51(18)	74.67(13)	74.4(2)
O13-Ln-N10	67.12(16)	67.18(14)	67.23(17)	67.50(12)	67.6(2)
O25-Ln-N10	137.20(17)	137.23(15)	137.31(19)	137.07(13)	137.3(2)
O15-Ln-N10	63.83(17)	63.86(15)	63.67(18)	64.20(12)	64.2(2)
O11-Ln-N10	64.27(17)	64.63(15)	64.91(19)	65.11(13)	65.6(2)
O21-Ln-N10	137.99(18)	137.63(16)	137.11(19)	136.97(14)	136.6(2)
OW1-Ln-N10	112.34(16)	112.33(14)	112.13(17)	112.14(12)	112.3(2)
N20-Ln-N10	123.56(17)	123.74(16)	124.05(18)	124.01(13)	124.3(2)

0.080 Å above their mean plane, respectively, while the N10 and Ow1 atoms are displaced in the opposite direction by 0.084-0.088 and 0.081-0.084 Å, respectively. These displacements from the mean planes are due to the heterogeneous coordinating atoms. Even for the upper plane constituted by the four oxygen atoms, the O21, O23 and O25 oxygen atoms belong to the three carboxylic groups atoms attached to the N20 atom, while O11 belongs to the other NTA. These polyhedrons indicate that the [Ln(NTA)$_2$·H$_2$O]$^{3-}$ complexes form a slightly distorted CSAP geometry and possess a C_{2v} point group rather than a C_{4v}.

Characterization of luminescence. The PL, luminescence and excitation spectra of the complexes were measured at various temperature. As shown in Figure 2(a),

Table 3. Average bond lengths (Å) of Ln(III) complexes with NTA and crystal ionic radii of Ln(III)

Ln	formula	Ln-N	Ln-O	ionic radius[a]	ref.
Pr	$Pr{\cdot}NTA{\cdot}H_2O$	2.68(2)	2.47(2)	1.013	b
Sm	$K_3[Sm(NTA)_2(H_2O)]{\cdot}5.5H_2O$	2.672(5)	2.425(5)	0.964	this work
Eu	$K_3[Eu(NTA)_2(H_2O)]{\cdot}5.5H_2O$	2.666(5)	2.411(4)	0.950	this work
Gd	$K_3[Gd(NTA)_2(H_2O)]{\cdot}5.5H_2O$	2.657(6)	2.403(5)	0.938	this work
Tb	$KNa_2[Tb(NTA)_2{\cdot}H_2O]{\cdot}5.5H_2O$	2.649(4)	2.383(3)	0.923	this work
Dy	$Dy{\cdot}NTA{\cdot}2H_2O$	2.578(8)	2.345(10)	0.908	c
Ho	$K_3[Ho(NTA)_2(H_2O)]{\cdot}5.5H_2O$	2.632(7)	2.366(7)	0.894	this work
Tm	$[Tm(NTA){\cdot}(H_2O)_2]{\cdot}2H_2O$	2.543(13)	2.305(9)	0.869	d

a: 14, b: 4, c: 5, d: 6.

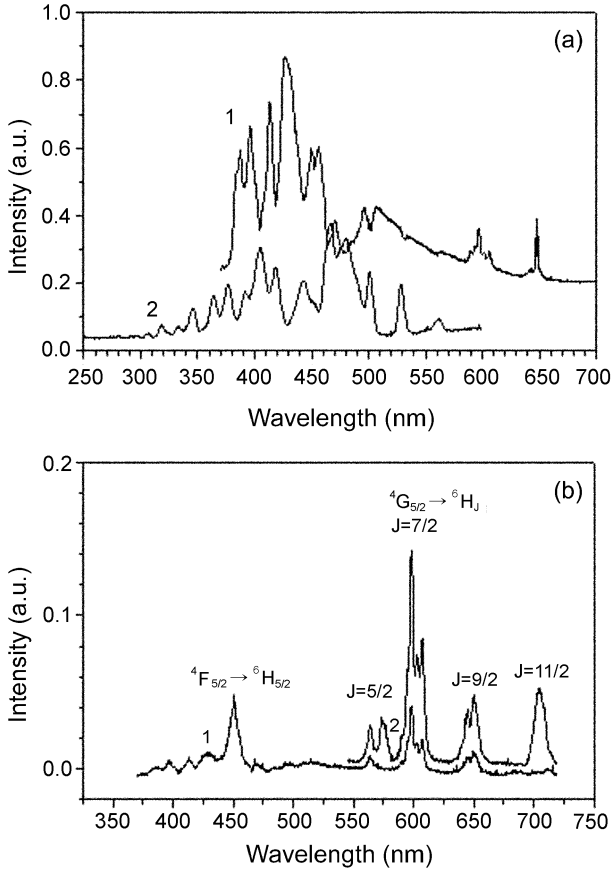

Figure 2. (a) PL (1; RT), excitation (2; λ_{ems} = 649 nm, T = 10 K) and (b) luminescence (λ_{exc} = 1; 346 nm, 2; 468 nm, RT) spectra of $[Sm(NTA)_2{\cdot}H_2O]^{3-}$.

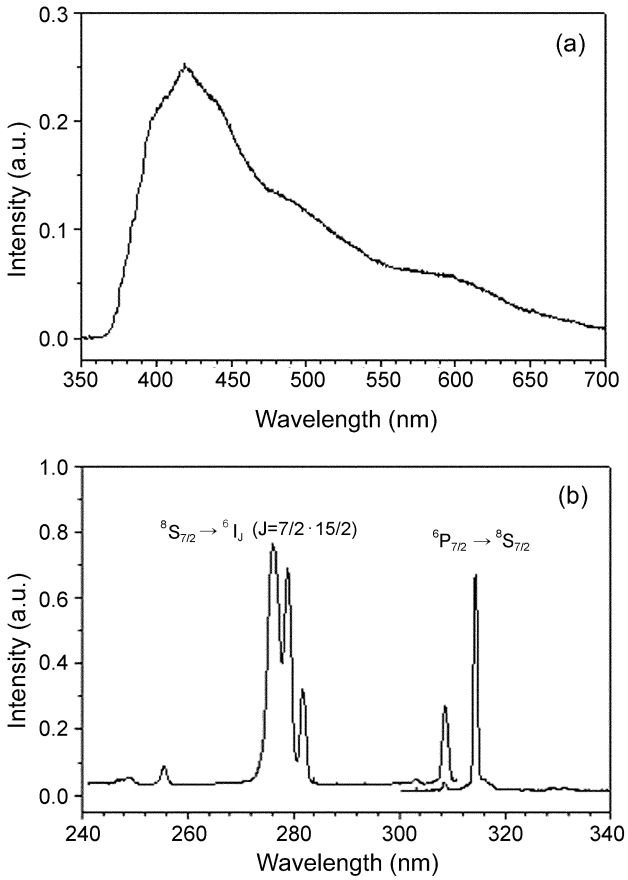

Figure 3. (a) PL and (b) emission (λ_{exn} = 276 nm) and excitation (λ_{ems} = 314.4 nm) spectra of $[Gd(NTA)_2{\cdot}H_2O]^{3-}$ (RT).

for $[Sm(NTA)_2{\cdot}H_2O]^{3-}$, the 325 nm excitation produced a very complicate PL spectrum spanning over the UV-visible region. The PL spectrum consists of a broad band spanning over 300-700 nm region and some sharp lines in the low-energy region. The luminescence of $[Sm(NTA)_2{\cdot}H_2O]^{3-}$ was also investigated as a function of an exciting photon energy. As shown in Figure 2(b), the 346 nm excitation produces four weak bands, peaking at 450.5, 565.0, 598.7 and 650.5 nm, accompanying very weak satellite bands in the high-energy side. The 468 nm excitation produces the strongest emission from Sm(III) in the 550-720 nm region, arising from the transitions from the emitting $^4G_{5/2}$ level to the ground ^6H_J levels. The broad band, which are not originated from Sm(III), may be responsible for the intraligand emission. It can be confirmed by the PL spectrum of $[Gd(NTA)_2{\cdot}H_2O]^{3-}$, since the first excited $^6P_{7/2}$ state of Gd(III) is higher than the 325 nm excitating energy. As shown in Figure 3(a), the intraligand emission appeared in the 350-700 nm region is typical fluorescence and phosphorescence, which are responsible for the $^{1,3}\tilde{A} \rightarrow {}^1\tilde{X}$ transitions of the carbony group of NTA, respectively. For $[Sm(NTA)_2{\cdot}H_2O]^{3-}$, however, there is a series of spectral dips in the emission profile. To examine whether these dips are associated with the Sm(III) ion in the complex, the excitation spectrum of the

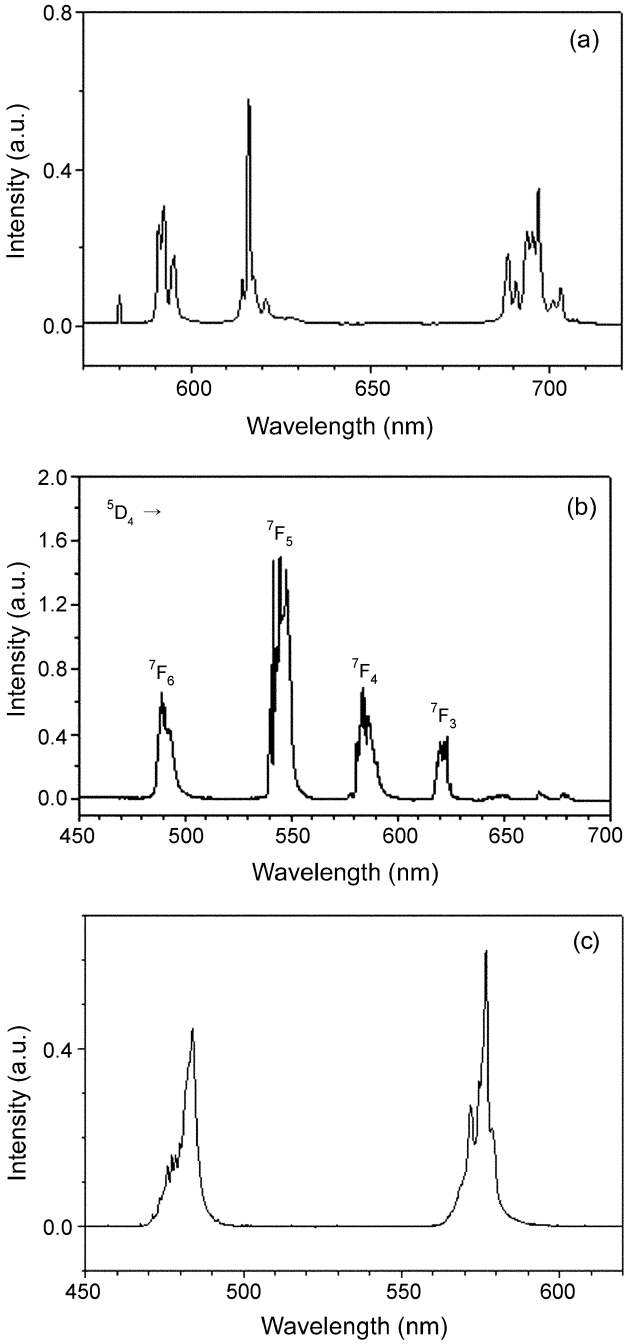

Figure 4. PL spectra of : (a) [Eu(NTA)$_2$·H$_2$O]$^{3-}$ (T = 10 K), (b) [Tb(NTA)$_2$·H$_2$O]$^{3-}$ (T = 10 K) and (c) [Dy(NTA)$_2$·H$_2$O]$^{3-}$ (T = 78.8 K).

649 nm emission was measured at 10 K. As shown in Figure 2(a), the peaks of the excitation bands coincide exactly with the locations of the spectral dips. This result indicates that the spectral dips in the intraligand luminescence profile arise from the radiative energy transfer (RET) from the ligand to the Sm(III) ion. The nonradiative energy transfer (NRET) band from NTA to Sm(III) did not appear in the excitation spectrum. As illustrated in Figures 3(b), for [Gd(NTA)$_2$·H$_2$O]$^{3-}$, the 276 nm excitation produced a strong emission band, peaking at 314.4 nm, and some satellite bands. These bands can be assigned as the $^6P_{7/2} \rightarrow {}^8S_{7/2}$ transition. There are three strong bands peaking at 280.6, 277.7 and 274.9 nm in the excitation spectrum. These three bands can be attributed to the transitions from the ground state to the degenerate ^6I_J (J = 7/2 15/2) states. The [Ho(NTA)$_2$·H$_2$O]$^{3-}$ complex produced only the intraligand luminescence with a series of spectral holes.

The complexes of [Eu(NTA)$_2$·H$_2$O]$^{3-}$, [Tb(NTA)$_2$·H$_2$O]$^{3-}$ and [Dy(NTA)$_2$·H$_2$O]$^{3-}$ excited at 325 nm produce very bright red, green and greenish yellow luminescence, respectively. The PL lines, shown in Figure 4, are very typical features, arising mostly from the $^5D_0 \rightarrow {}^7F_J$ (J = 1, 2, 3, 4), the $^5D_4 \rightarrow {}^7F_J$ (J = 6, 5, 4, 3) and the $^4F_{9/2} \rightarrow {}^6H_J$ (J = 15/2 and 13/2) transitions, respectively. Previously,[12] the observed luminescence lines for [Eu(NTA)$_2$·H$_2$O]$^{3-}$ and [Tb(NTA)$_2$·H$_2$O]$^{3-}$ were characterized in the framework of the crystal-field Hamiltonian with C_{2v} site symmetry. The set of refined crystal-field parameters under the C_{2v} site symmetry of the two ions satisfactorily produced good fits between calculated and experimentally observed energy-level structures. However, for [Dy(NTA)$_2$·H$_2$O]$^{3-}$, the number of the observed lines is not enough to refine the nine crystal-field parameters. In this study, the absolute quantum yields of these three complexes were precisely determined at room temperature upon a 325-nm excitation: Q = 0.63(±0), 5.9(±0.26) and 6.3(±0.15) % for [Eu(NTA)$_2$·H$_2$O]$^{3-}$, [Tb(NTA)$_2$·H$_2$O]$^{3-}$ and [Dy(NTA)$_2$·H$_2$O]$^{3-}$, respectively. Of the lanthanide metal ions, Eu^{3+} and Tb^{3+} ions are known to have hypersensitivity to the coordination environment and to show an efficient electroluminescence.[13] The Tb(III) and Dy(III) complexes, however, are much more luminescent than the Eu(III) complex. Surprisingly, the luminescence of [Dy(NTA)$_2$·H$_2$O]$^{3-}$ is more effective than that of the hypersensitive Tb(III).

Supplementary material. Crystallographic data for the structures reported here have been deposited with the Cambridge Crystallographic Data Centre (Deposition No. CCDC-23360-233634). The data can be obtained free of charge *via www.ccdc.cam.ac.uk/conts/retriveing.html* (or from the CCDC, 12 Union Road, Cambridge CB2 1EZ, UK; fax: +44 1223 336033; e-mail: deposit@ccdc.cam.ac.uk).

Acknowledgements. This work was supported by the Korea Science and Engineering Foundation (KOSEF R01-2001-00055) and Chungnam National University (2001-2002).

References

1. Huskens, J.; Kennedy, A. D.; van Bekkum, H.; Peters, J. A. *J. Am. Chem. Soc.* **1995**, *117*, 375.
2. Yokoyama, Y.; Asami, T.; Kanesato, M.; Suzuki, T. M. *Chem. Lett.* **1993**, 383.
3. Inoue, Y.; Kumagai, H.; Shimomura, Y.; Yokoyama, T.; Suzuki, T. M. *Anal. Chem.* **1996**, *69*, 1517.
4. Martin, L.; Jacobson, R. A. *Inorg. Chem.* **1972**, *11*, 2785.
5. Martin, L.; Jacobson, R. A. *Inorg. Chem.* **1972**, *11*, 2789.
6. Chen, Y.; Ma, B.-Q.; Liu, Q.-D.; Li, J.-R.; Gao, S. *Inorg. Chem.*

Comm. **2000**, *3*, 319.
7. *SHELXTL, 5.030*; Brucker Analytical X-ray Instruments, Inc.: Madison, WI, 1998.
8. Sheldrick, G. M. *SHELEX97*; Institute fuer Anorganiscche Chemie der Universitaet: Göttingen, Germany, 1998.
9. de Mello, J. C.; Wittmann, H. F.; Friend, R. H. *Adv. Mater.* **1997**, *9*, 230.
10. Drew, M. G. B. *Coord. Chem. Rev.* **1977**, *24*, 179.
11. Thompson, L. C. In *Handbook on the Physics and Chemistry of Rare Earth*; Gschneider, K. A. Jr.; Eyring, L., Eds.; Elsevier; North-Holland, Amsterdam, New York, Oxford, 1979; Vol 3, Chapter, 25.
12. Kang, J.-G.; Hong, J.-P.; Yoon, S.-K.; Bae, J.-H.; Kim, Y.-D. *J. Alloys Comp.* **2002**, *339*, 248.
13. You, B.; Kim, H. J.; Park, N. G.; Kim, Y. S. *Bull. Korean Chem. Soc.* **2001**, *22*, 1005.
14. Templet, D. H.; Dauben, C. H. *J. Am. Chem. Soc.* **1954**, *76*, 5237.